

Hydrogen-bonded clusters of 1,1'-ferrocenedicarboxylic acid on Au(111) are initially formed in solution

Rebecca C. Quardokus,¹ Natalie A. Wasio,¹ Ryan D. Brown,¹ John A. Christie,¹ Kenneth W. Henderson,¹ Ryan P. Forrest,¹ Craig S. Lent,² Steven A. Corcelli,¹ and S. Alex Kandel^{1,a)}

¹Department of Chemistry and Biochemistry, University of Notre Dame, Notre Dame, Indiana 46556-5670, USA

²Department of Electrical Engineering, University of Notre Dame, Notre Dame, Indiana 46556-5637, USA

(Received 30 November 2014; accepted 4 February 2015; published online 25 February 2015)

Low-temperature scanning tunneling microscopy is used to observe self-assembled structures of ferrocenedicarboxylic acid ($\text{Fc}(\text{COOH})_2$) on the Au(111) surface. The surface is prepared by pulse-deposition of $\text{Fc}(\text{COOH})_2$ dissolved in methanol, and the solvent is evaporated before imaging. While the rows of hydrogen-bonded dimers that are common for carboxylic acid species are observed, the majority of adsorbed $\text{Fc}(\text{COOH})_2$ is instead found in six-molecule clusters with a well-defined and chiral geometry. The coverage and distribution of these clusters are consistent with a random sequential adsorption model, showing that solution-phase species are determinative of adsorbate distribution for this system under these reaction conditions. © 2015 AIP Publishing LLC. [<http://dx.doi.org/10.1063/1.4909517>]

INTRODUCTION

Strong covalent or ionic bonding is characteristic of the structures of most bulk inorganic materials. Bonding networks in these materials can be simple (single-crystal metals or salts) or complex (e.g., paulingite¹ or other zeolites). Typically, inorganic compounds can be defined in terms of a unit cell and translational symmetry defined by a lattice group; however, the presence of strong interatomic bonding means that there is only an indirect connection between the bulk material properties and the atomic composition and properties of the unit cell. In contrast, organic compounds (including organometallics, polymers, and composites) are formed from covalently bound molecules that are packed and ordered by relatively weaker non-covalent interactions. This hierarchy of energy scales means that bulk properties can derive from the component molecules, from the extended network, or from both. This also results in a degree of separability between short-range composition and long-range order. The research areas of crystal engineering and supramolecular assembly are based upon leveraging the understanding of intermolecular interactions to create extended materials with desired structures and, therefore, desired properties.² Conversely, advances in these fields have led to a systematic exploration of the interrelationship between molecular structure and long-range order, which in turn can potentially lead to new insights into the processes of crystal nucleation and growth.

Self-assembled monolayers are created by the exposure of a surface to one or more molecular adsorbates to produce ordered, well-characterized thin films—self-assembly

can thus be seen as the application of ideas of crystal engineering and supramolecular chemistry to produce materials that are confined in two dimensions.³ Self-assembly is distinguished from epitaxial growth by the presence of strong intramolecular (covalent) bonds and much weaker intermolecular interactions. Molecular-substrate interactions can range from weak to strong in self-assembly, though when adsorbates are strongly bound to a surface, mobility is generally necessary to allow for the formation of order without kinetic traps.

Hydrogen bonding is one of the most powerful and versatile tools in the supramolecular chemist's toolbox.⁴⁻⁷ This is partly because hydrogen bonds are relatively strong non-covalent interactions, but also because the term encompasses interactions between a very wide range of donor and acceptor species at different geometries. In three-dimensional systems, hydrogen bonds have been extensively characterized through quantitative analysis of solid-state crystal structures. This has led to a variety of established supramolecular “synthons”—pairs of functional groups with known interaction strengths and binding geometry that can be used to facilitate the desired supramolecular assembly.⁸

Hydrogen bonding is also used to produce desired structures in self-assembled monolayers.⁹⁻¹⁹ Perhaps, the most widely used synthon in surface self-assembly is the carboxylic acid dimer, in which adjacent COOH groups form two strong hydrogen bonds, with each OH acting as a donor and each C=O as an acceptor. Molecules with one or more COOH groups in various geometries have been used to create patterning in one and two dimensions.

Potential new structures arising from alternate hydrogen-bonding motifs have been less thoroughly explored in surface-adsorbate systems than in three-dimensional supramolecular chemistry. In particular, molecules with more than one H-bond

^{a)} Author to whom correspondence should be addressed. Electronic mail: skandel@nd.edu

donor and/or acceptor can explore a rich configurational space with multiple local minima, potentially forming structures significantly different than those created when only a single synthon is present.^{20–24}

Here, we describe the deposition of ferrocenedicarboxylic acid ($\text{Fc}(\text{COOH})_2$) from solution onto clean Au(111) surfaces. We have previously found that ferrocene with a single COOH group (FcCOOH) forms a variety of complex structures due to the combination of strong COOH-derived hydrogen bonding with C-H \cdots O hydrogen bonding; these structures include a cyclic pentamer that assembles aperiodically at high surface coverage to make a two-dimensional quasicrystal.²⁵ At lower coverage, FcCOOH forms isolated cyclic pentamers, as well as paired-row clusters containing 4–12 molecules.²⁶ The distribution of cluster sizes is highly peaked, more so than is consistent with a binomial distribution. These statistics are difficult to explain as the result of cluster formation and growth on the surface, and we suggested that molecular clusters instead were forming in solution and depositing intact. Scanning tunneling microscopy (STM) images of $\text{Fc}(\text{COOH})_2$ presented here show that nearly all of these molecules are observed in six-member clusters, both at low and at high surface coverage. The experimental data are consistent with formation of these clusters in solution, followed by adsorption without further surface diffusion. Other simple mechanisms do not adequately explain the observations.

EXPERIMENTAL

Sample preparation and STM

Gold-on-mica Au(111) surfaces were cleaned in vacuum using with two cycles of argon-sputtering (6 mA, 30 min) and annealing (700 K, 20 min). The sample was then moved to the deposition chamber. Deposition was from a 7 mM methanol solution of 1,1'-ferrocenedicarboxylic acid ($\text{Fc}(\text{COOH})_2$) (Fig. 1) prepared in an argon-purged glovebox. Microliters of solution were transferred to the surface using a pulsed-solenoid valve (Parker Instruments 9-series, 0.5 mm nozzle diameter, IOTA One driver); three 0.5 ms pulses created significant coverage for imaging, with no multilayer formation evident.

Sample and solution were maintained at room temperature throughout the sample preparation process. Solvent was allowed to evaporate at room temperature, with no further annealing done. After the deposition-chamber pressure had returned to baseline, the sample was transferred into the

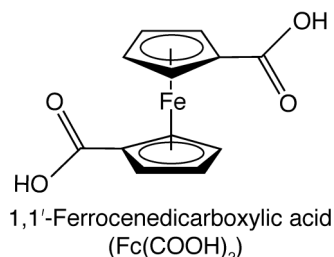


FIG. 1. Molecular structure of 1,1'-ferrocenedicarboxylic acid ($\text{Fc}(\text{COOH})_2$).

UHV chamber and placed into the stage of an Omicron LT-STM operating at 77 K. All STM images were acquired in constant-current mode.

$\text{Fc}(\text{COOH})_2$ synthesis

All manipulations were carried out using standard Schlenk techniques under a nitrogen (N_2) atmosphere. Unless otherwise mentioned, reagents and solvents were used as received. NMR spectra were recorded on a Bruker-500 spectrometer at 293 K and were referenced internally to the residual signals of the deuterated solvent. Ether was purified by passage through a solvent purification system (Innovative Technology). Tetramethylethylenediamine (TMEDA) was distilled from CaH_2 and stored on 4 Å sieves. Synthesis of 1,1'-ferrocenedicarboxylic acid follows a modified literature procedure.²⁷

Et_2O (5 mL) and TMEDA (2.43 mL, 16.2 mmol) were mixed in a flame dried 50 mL Schlenk flask. The flask was cooled in an ice bath, and a 2.5 M hexane solution of nBuLi (6.46 mL, 16.15 mmol) was added to the contents. The solution was allowed to warm to room temperature while stirring. A second, flame dried 50 mL Schlenk flask was charged with ferrocene (1 g, 5.4 mmol) and Et_2O (5 mL). The bright orange ferrocene solution was cannulated to the nBuLi /TMEDA solution and the mixture was allowed to stir for 24 h. The following day CO_2 was bubbled through the solution at -78°C for 3 h before being warmed to room temperature and subsequently quenched with 20 mL H_2O . The mixture was acidified with 6 M HCl, resulting in a bright orange precipitate. This precipitate was collected via filtration and washed with H_2O and methylene chloride to yield pure 1,1'-ferrocenedicarboxylic acid (0.338 g, 23%). NMR spectroscopy agrees with published data.²⁸ ^1H NMR ($\text{DMSO}-d_6$, 500 MHz) δ 4.45 (t, 4H), 4.69 (t, 4H), 12.32 (br s, 2H) ppm. ^{13}C NMR ($\text{DMSO}-d_6$, 125.77 MHz): δ 71.27, 72.56, 73.46, 171.04 ppm.

RESULTS AND DISCUSSION

Pulsed-deposition of $\text{Fc}(\text{COOH})_2$ in methanol onto Au(111) results in a heterogeneous surface containing molecular clusters of various sizes and structures. Representative images of the structures typically observed on this surface are presented in Fig. 2. The assembly of $\text{Fc}(\text{COOH})_2$ molecules on the Au(111) surface appears to contain three distinct classes of structures: dimer rows, hexamer clusters, and disordered molecules. The dimer rows appear to be pairs of $\text{Fc}(\text{COOH})_2$ molecules stacked alongside other dimers, which forms long rows. The hexamers are chiral structures consisting of six molecules, and these structures do not appear to propagate beyond the six molecules. The majority of five-molecule clusters actually have the internal structure of the hexamer, but have a vacancy, and thus are defective hexamers rather than a unique structure. Similarly, clusters of seven or eight molecules consist of a central hexamer with “disordered” molecules attached to the exterior of the hexamer. The images have many features which are not clearly assigned, but a reasonable assumption would be that the disordered regions consist of solvent from the pulse deposition,^{29,30} as well as

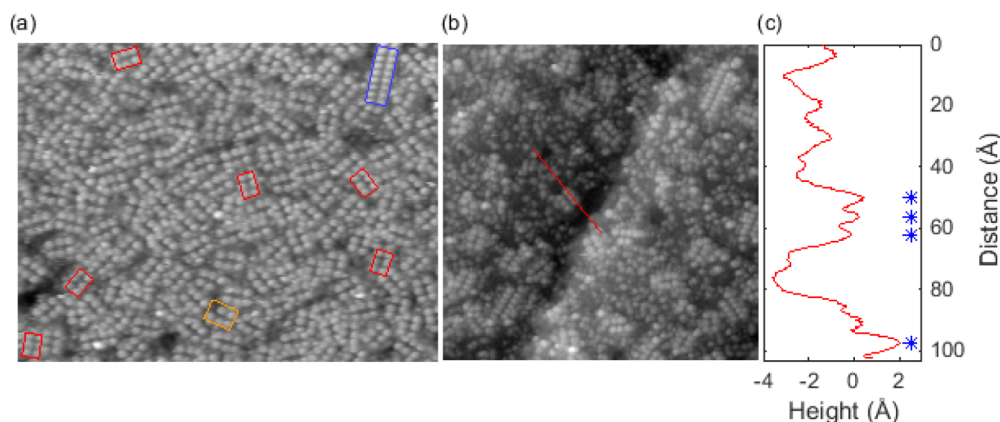


FIG. 2. A $325 \times 245 \text{ \AA}$ image obtained at a surface temperature of 77 K using a sample bias of +1.0 V and a tunneling current of 10 pA depicts a typical high-coverage region of the surface, (a). The blue box highlights a dimer row, the red boxes show the position of a small sampling of the hexamers present in this region, and the orange box highlights the position of a five molecule cluster having the structure of a defective hexamer. The hexamer structure is the dominate form observed in this image. A $297 \times 297 \text{ \AA}$ image obtained at 77 K with a sample bias of +0.5 V and a tunneling current of 10 pA which shows a region of this surface with a lower density $\text{Fc}(\text{COOH})_2$ coverage, (b). The red line corresponds to the line scan displayed in (c), and the blue asterisks in (c) show the positions of upright $\text{Fc}(\text{COOH})_2$ molecules.

molecules with orientations in which the molecular axis is tilted away from the surface normal.^{25,31}

In order to characterize the internal structure of the hexamers, the position of each molecule within the hexamer relative to the cluster centroid was recorded for each clearly and completely resolved hexamer in the images. These positions were sorted by the chiral conformations (labeled “S” and “Z”), when that assignment was possible, then averaged. The average positions of the molecules within the Z and S hexamers are presented in Table I, and scatter plots of these data are presented in Figs. 3(a) and 3(b). The average positions of molecules within the two types of hexamers also give the average separation between molecules, and those data are presented in Table II. Composite hexamer images were constructed from the topography image in Fig. 2 and are shown in Figs. 3(c) and 3(d) for the S and Z hexamers, respectively. Out of a total of 173 hexamer clusters identified in the images, we found 90 S enantiomers (53.76%) and 83 Z enantiomers (46.24%), which is consistent with a racemic mixture being present on the surface. There is clearly strong positional order within the hexamers, and it is also evident, from the data and composite images, that this structure does not propagate beyond the core six molecules.

TABLE I. The average position of each molecule in the S (left) and Z (right) enantiomers relative to the centroid of the hexamer. All positions are given in \AA . The alphabetic labels for the molecular positions within the hexamer are shown in Fig. 4.

Molecule	S		Z	
	<i>x</i>	<i>y</i>	<i>x</i>	<i>y</i>
A	-6.9 ± 0.4	3.8 ± 0.3	-7.0 ± 0.4	4.0 ± 0.4
B	0.6 ± 0.3	4.4 ± 0.3	-0.7 ± 0.3	4.5 ± 0.3
C	7.0 ± 0.3	4.0 ± 0.3	6.8 ± 0.4	3.9 ± 0.4
D	-7.0 ± 0.4	-4.1 ± 0.3	-6.9 ± 0.4	-4.1 ± 0.4
E	-0.6 ± 0.3	4.4 ± 0.3	0.7 ± 0.4	-4.4 ± 0.3
F	6.8 ± 0.4	-3.8 ± 0.3	7.1 ± 0.5	-3.9 ± 0.3

Before discussing the specific aspects of these surface structures, it is useful to consider the bulk crystal structures of $\text{Fc}(\text{COOH})_2$. Three solid state crystal polymorphs of 1,1'-ferrocenedicarboxylic acid have been reported in the literature.^{32–34} Each structure is comprised of $\text{Fc}(\text{COOH})_2$ dimers in which both carboxylic acid groups of one molecule form hydrogen bonds with those of the second molecule, resulting in a total of four hydrogen bonds per dimer. The main difference between the crystal polymorphs is in the relative orientation of neighboring dimers. In all three bulk crystal structures, the distance between the iron atoms, or cyclopentadiene centroids, of a dimer pair is 9.1 \AA , which is consistent with both the spacing between the pulse-deposited dimer rows as well as the spacing between molecules “B” and “E” in the two hexamer forms (Table II). There is no analogous structure in the bulk crystal to the hexamer clusters observed on the surface, and to the best of our knowledge, no report of chiral structures within $\text{Fc}(\text{COOH})_2$ crystals.

Based on the solid-state structure of $\text{Fc}(\text{COOH})_2$, the general behavior of surface-adsorbed carboxylic acids, and the observation of some dimer-row features in our images, it is likely that dimer rows are indeed the minimum-energy configuration for adsorbed $\text{Fc}(\text{COOH})_2$, and that the hexamer structure is a metastable one. Adsorption conditions are dictated by the rapid solvent evaporation that occurs during the pulse deposition process, and it is not surprising that these conditions allow metastable structure formation.^{35,36}

The exact molecular structure of a hexamer cannot be determined directly from STM images, although the brightness of the features indicates that each molecule is adsorbed with the ferrocene Cp planes parallel to the surface; faint intramolecular π structure can be seen in Fig. 3 that confirms this assignment. Next, the analysis of internal molecule-molecule distances in Table II shows that within each hexamer, only a single distance (B–E) is consistent with full COOH–COOH dimerization. Despite this fact, the formation of this chiral hexamer structure is clearly very favorable during our deposition, given that a strong majority of the molecules imaged and clusters observed are hexamers.

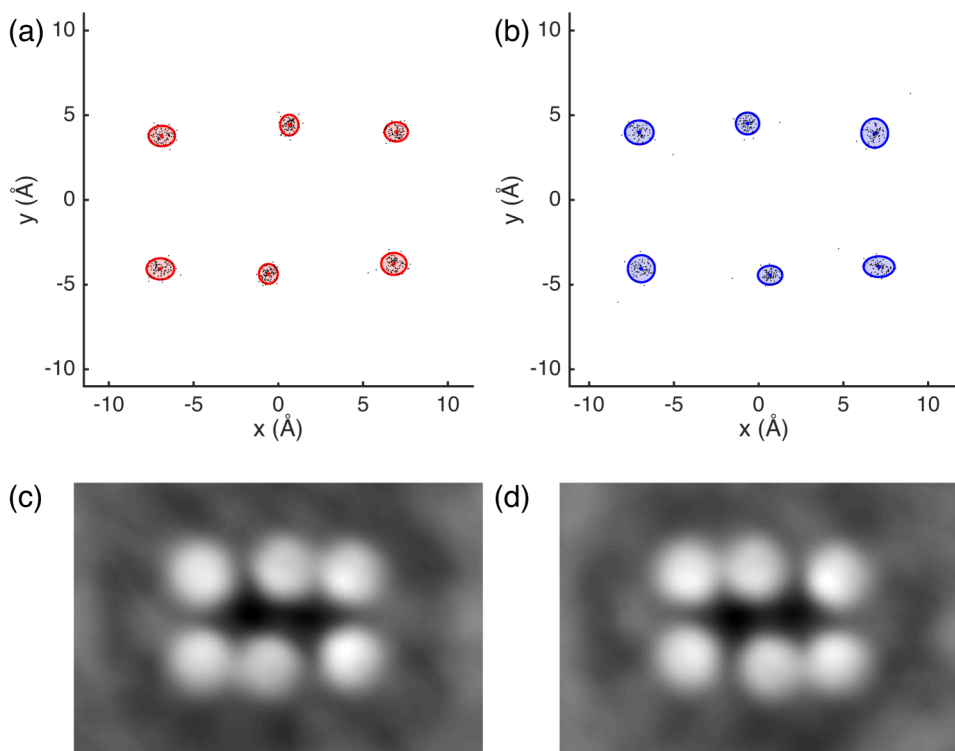


FIG. 3. The relative position of each molecule within each hexamer for the “S,” (a) and “Z,” (b), enantiomers (black dots). The red (blue) dots are the average positions, and the red (blue) circles are twice the standard deviation of the molecular positions for the S (Z) enantiomer. Panels (c) and (d) are composite images of the S and Z enantiomers, respectively, obtained from the image presented in Figure 2.

Finally, the fact that the hexamers do not appear to form larger structures, or even impose much order on adjacent clusters, seems to indicate that these clusters do not have H-bonding interactions with neighboring molecules or clusters. The only reasonable explanation for why this occurs is that none of the six molecules have outward facing carboxylic acid groups, as seen in Fig. 4(b). Without electronic structure calculations, any argument for how bonding within the hexamer leads to a metastable state is necessarily speculative. However, it is not unreasonable to expect this structure to involve weak hydrogen bonding between carboxylic acid groups and α -carbon hydrogens from a neighboring cyclopentadiene ring, as in the case of FcCOOH.²⁵

The hexamers in Fig. 2 are packed at high density, but without apparent aggregation. There are two possible models that could explain the presence of the chiral hexamers on this surface. The first model involves the adsorption of Fc(COOH)₂ on the surface, followed by a nucleation and growth process. It is difficult to explain how the observed structures can result from an adsorption, nucleation, and growth process on

the surface since this mechanism is necessarily driven by a fairly complex combination of factors. Either individual Fc(COOH)₂ molecules or dimers must adsorb and retain some mobility on the surface in order to diffuse and eventually form clusters. This diffusion can happen spontaneously or be assisted by a thin evaporating film of solvent, which itself can exhibit complex behaviors.^{37–39} There must exist a deep free-energy minimum, or “magic number” configuration,^{40,41} for chiral hexamer clusters on the surface. Since hexamers

TABLE II. The distances between molecules in the S (left) and Z (right) enantiomer. All distances are given in Å. The alphabetic labels for the molecular positions within the hexamer are shown in Fig. 4.

	S	Z
	Distance	Distance
A–D	7.8 ± 0.7	8.0 ± 0.8
A–B	7.5 ± 0.6	6.4 ± 0.7
D–E	6.3 ± 0.7	7.6 ± 0.7
B–E	8.9 ± 0.6	9.1 ± 0.7
B–D	11.4 ± 0.7	10.6 ± 0.7
B–F	10.3 ± 0.6	11.5 ± 0.7

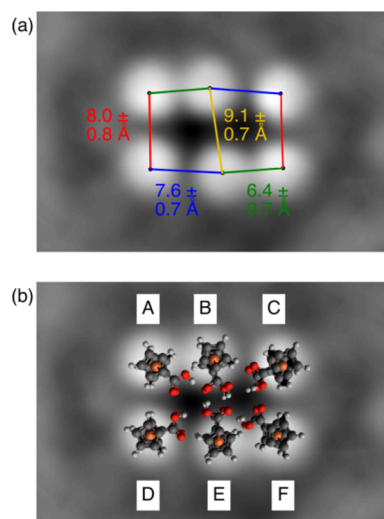


FIG. 4. The Z enantiomer of the hexamer is shown with critical distances labeled, (a), and with a depiction of the likely orientation of the molecules within the hexamer based on the STM data. We assume that the top and bottom rings of the ferrocene have the same orientation as in the bulk crystal structure, but this need not be the actual conformation at this interface. The six hexamer molecules are labeled A–F for discussion of positions and distances in panel (b).

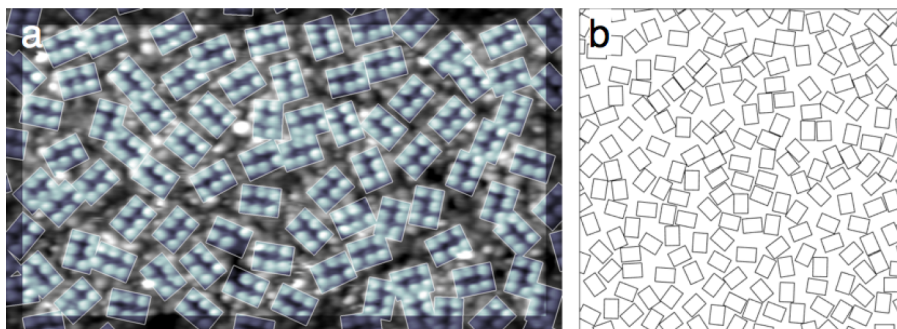


FIG. 5. (a) Cropped area from Fig. 2, showing details of the coverage analysis. The area assigned to each hexamer is outlined by a white rectangle, and edge effects are avoided by excluding a small area around the perimeter of the analyzed area. (b) Arrangement of rectangles with 3:2.2 aspect ratio determined in the jamming limit of random sequential adsorption.

are present at high coverages, see Fig. 2, the relatively low frequency of “orphan” molecules or small clusters requires some mechanism by which individual molecules or small clusters can diffuse out of regions where the hexamers appear to have jammed packing, and thus continue nucleating and growing. Finally, if the jamming is relieved by hexamer mobility (which is later quenched by sample cooling), the interactions between hexamers must be sufficiently weak such that no strong ordering of neighboring hexamers is observed. It is possible that all of these conditions exist in our system, the data do not exclude such a possibility, but we feel that another model presents an explanation of the observed surface structures and packing by making a much simpler set of assumptions.

We suggest that this simpler model is one in which cluster formation occurs in solution, and that the packing of the hexamers on the surface is driven by random sequential adsorption (RSA). For this mechanism to be valid some fairly simple conditions must exist in this system. The hexamers must exist in solution at some point during the deposition and drying process. Electrospray mass spectrometry experiments of $\text{Fc}(\text{COOH})_2$ in methanol did observe the formation of tetramers in the presence of alkali cations,⁴² but no direct evidence exists to corroborate the presence of neutral hexamer clusters of ferrocendicarboxylic acid in solution. However, the experimental conditions were quite different from those employed during our deposition, and it is reasonable to expect that neutral clusters of hydrogen bonding molecules can form in the aerosol droplets as has been observed in simpler molecular systems.^{43–45} The hexamers need not be a majority species, and the presence of metastable molecular clusters is possible in the non-equilibrium conditions that can exist in a aerosol droplet undergoing evaporation^{35,36} or a thin evaporating film of solvent.³⁷ Once these metastable species form, they come out of solution as predicted by Ostwald’s rule, which states that less-stable species will precipitate out of solution prior to more-stable structures.^{46,47} These clusters then adsorb intact but experience no further change in cluster size or orientation, so that the distances and relative orientation of neighboring clusters arise solely from statistical and geometric factors.

Random sequential adsorption has been well modeled in the literature. In particular, Vigil and Ziff characterized the sequential adsorption of rectangles, starting with an empty surface and continuing until maximal “jammed” coverage, and assuming no interaction between rectangles other than prohibition of overlap.⁴⁸ The characteristics of jammed

surfaces are highly similar to the experimental structure observed in Fig. 2. Figures 5 and 6 present a comparison of the STM data to a RSA model. The simplicity of this model arises from the fact that cluster formation occurs in the non-equilibrium conditions in the solvent droplets prior to deposition, and thus avoids the complicated explanations for how such high density, nearly mono-disperse clusters can form on the surface.

The experimental hexamer coverage is determined to be 0.55 for the area shown in Fig. 5, though this number depends on the precise definition of cluster shape and size and can vary by up to 0.1. This matches the prediction of RSA for rectangles with a 3:2.2 aspect ratio, which is 0.54.⁴⁸ The general features of cluster arrangement also appear qualitatively similar when comparing the experiment (Fig. 5(a)) to the RSA simulation (Fig. 5(b)). The relative position and orientation of neighboring clusters are analyzed through 2-D and 1-D correlation functions and shown in Fig. 6; again, the experimental data match the predictions of the model well. These data are strongly consistent with random sequential adsorption of hexamer clusters which form in solution during the deposition process. However, these data do not conclusively indicate the exact mechanism by which hexamers form in the solvent droplets, the environment of the evaporating droplets themselves, how these molecular clusters precipitate out of solution, and the fate of clusters which can not be accommodated into regions exhibiting maximal coverage.

The self-assembly behavior of pulse deposited $\text{Fc}(\text{COOH})_2$ in methanol is quite different from that observed in pulsed deposited FcCOOH in benzene.²⁶ The most surprising difference between these two studies was the absence of cyclic pentamers on the diacid surface, which was fully expected to be observed based on the results from the monoacid assembly, and the preponderance of chiral hexamers on the diacid surface which was not observed for FcCOOH . Methanol was used in place of benzene in the current experiment due to solubility concerns, so the differences in the structures observed between the two studies can easily result from the switch from a nonpolar solvent, benzene, to a polar solvent, methanol. It is difficult to determine an exact physical mechanism for the formation of specific cluster structures due to the use of different solvents in these studies, but there are some similarities worth discussing. Both studies found statistical distributions of cluster sizes inconsistent with the binomial distribution expected from an adsorption, nucleation, and growth model. The data support a

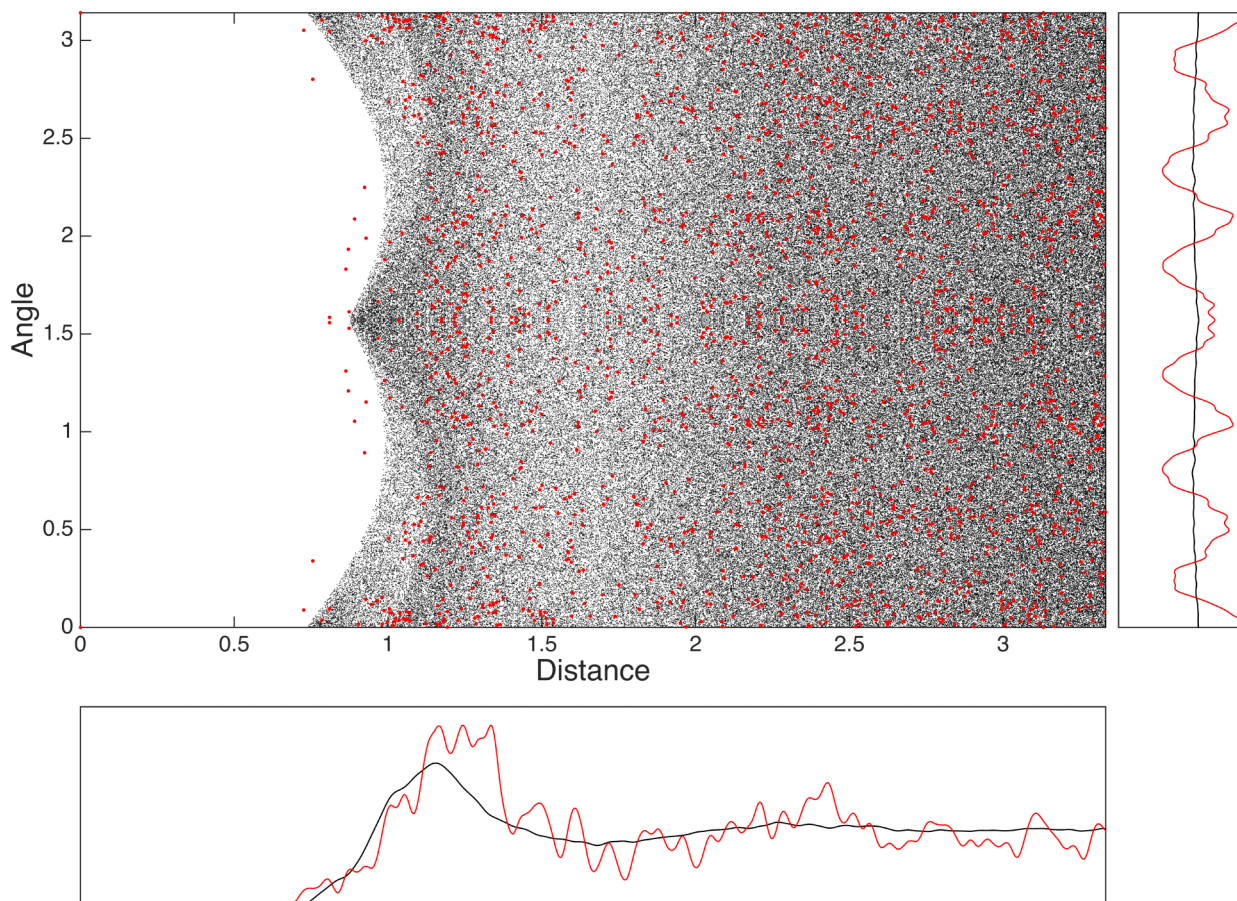


FIG. 6. Distance/angle correlation functions compared for simulated cluster positions assuming random sequential adsorption (black) and experimental cluster positions (red). Distance units are in multiples of the cluster long-axis dimension. Integrated correlation functions with respect to distance and angle are shown below and to the right. (Note that the experimental data show additional angular structure, likely due to the influence of the underlying substrate.)

model of cluster formation in solution followed by adsorption into a kinetically trapped configuration at the surface. The fact that this trend occurs for both non-polar and polar solvents strengthens the generality of our results, namely that cluster formation in solution can play an important role in the self-assembly of solution deposited molecules at an interface.

CONCLUSIONS

Pulsed deposition of a methanolic solution of 1,1'-ferrocenedicarboxylic acid onto a Au(111) interface results in the formation of chiral hexamer structures. These structures have no bulk analogue, having one internal H-bonding pair and four surrounding molecules with inward facing carboxylic acid groups; the structure is akin to inverse micelles. The high frequency of occurrence, random orientation, and coverage of the saturated surface all support the model of six-molecule cluster formation in the solvent during deposition followed by the random sequential adsorption of the clusters on the Au(111) interface, after which they can adopt the chiral hexamer structure.

The ability of metastable structures to transfer from solution to surface creates a link between solution and the solid state that has been proposed and investigated as a mechanism for the formation of three-dimensional crystal polymorphs.^{49–52} A similar link that allows the adsorption of

complex, metastable structures from solution potentially has broad relevance to the study of self-assembled monolayers.

ACKNOWLEDGMENTS

Support for this work has been provided by the National Science Foundation (NSF Grant No. CHE-1124762).

- ¹E. Gordon, S. Samson, and W. Kamb, "Crystal structure of zeolite paulingite," *Science* **154**, 1004–1007 (1966).
- ²M. D. Ward and P. R. Raithby, "Functional behaviour from controlled self-assembly: Challenges and prospects," *Chem. Soc. Rev.* **42**, 1619–1636 (2013).
- ³S. Whitelam, I. Tamblin, T. K. Haxton, M. B. Wieland, N. R. Champness, J. P. Garrahan, and P. H. Beton, "Common physical framework explains phase behavior and dynamics of atomic, molecular, and polymeric network formers," *Phys. Rev. X* **4**, 011044 (2014).
- ⁴C. Aakeroy and K. Seddon, "The hydrogen-bond and crystal engineering," *Chem. Soc. Rev.* **22**, 397–407 (1993).
- ⁵J. Bernstein, R. Davis, L. Shimoni, and N. Chang, "Patterns in hydrogen bonding—Functionality and graph set analysis in crystals," *Angew. Chem., Int. Ed.* **34**, 1555–1573 (1995).
- ⁶F. Allen, W. Motherwell, P. Raithby, G. Shields, and R. Taylor, "Systematic analysis of the probabilities of formation of bimolecular hydrogen-bonded ring motifs in organic crystal structures," *New J. Chem.* **23**, 25–34 (1999).
- ⁷T. Steiner, "The hydrogen bond in the solid state," *Angew. Chem., Int. Ed.* **41**, 48–76 (2002).
- ⁸G. Desiraju, "Supramolecular synthons in crystal engineering—a new organic-synthesis," *Angew. Chem., Int. Ed.* **34**, 2311–2327 (1995).
- ⁹M. E. Canas-Ventura, F. Klappenberger, S. Clair, S. Pons, K. Kern, H. Brune, T. Strunskus, C. Woell, R. Fasel, and J. V. Barth, "Coexistence of one- and

- two-dimensional supramolecular assemblies of terephthalic acid on Pd(111) due to self-limiting deprotonation," *J. Chem. Phys.* **125**, 184710 (2006).
- ¹⁰I. Cebula, E. F. Smith, M. d. C. Gimenez-Lopez, S. Yang, M. Schroeder, N. R. Champness, and P. H. Beton, "Packing of isophthalate tetracarboxylic acids on Au(111): Rows and disordered herringbone structures," *J. Phys. Chem. C* **117**, 18381–18385 (2013).
- ¹¹S. Clair, S. Pons, A. Seitsonen, H. Brune, K. Kern, and J. Barth, "STM study of terephthalic acid self-assembly on Au(111): Hydrogen-bonded sheets on an inhomogeneous substrate," *J. Phys. Chem. B* **108**, 14585–14590 (2004).
- ¹²C. Heininger, L. Kampschulte, W. Heckl, and M. Lackinger, "Distinct differences in self-assembly of aromatic linear dicarboxylic acids," *Langmuir* **25**, 968–972 (2009).
- ¹³L. Kampschulte, M. Lackinger, A. Maier, R. Kishore, S. Griessl, M. Schmitte, and W. Heckl, "Solvent induced polymorphism in supramolecular 1,3,5-benzenetricarboxylic acid monolayers," *J. Phys. Chem. B* **110**, 10829–10836 (2006).
- ¹⁴M. Lackinger and W. Heckl, "Carboxylic acids: Versatile building blocks and mediators for two-dimensional supramolecular self-assembly," *Langmuir* **25**, 11307–11321 (2009).
- ¹⁵Z. Pei, L. Lin, H. Zhang, L. Zhang, and Z. Xie, "Self-assembly of 2,6-naphthalenedicarboxylic acid and 4,4'-biphenyldicarboxylic acid on highly oriented pyrolytic graphite and Au(111) surfaces," *Electrochim. Acta* **55**, 8287–8292 (2010).
- ¹⁶L. Thomas, A. Kühnle, S. Rode, U. Beginn, and M. Reichling, "Monolayer structure of arachidic acid on graphite," *J. Phys. Chem. C* **114**, 18919–18924 (2010).
- ¹⁷A. G. Slater (nee Phillips), P. H. Beton, and N. R. Champness, "Two-dimensional supramolecular chemistry on surfaces," *Chem. Sci.* **2**, 1440–1448 (2011).
- ¹⁸R. Smith, P. Lewis, and P. Weiss, "Patterning self-assembled monolayers," *Prog. Surf. Sci.* **75**, 1–68 (2004).
- ¹⁹Y. Ye, W. Sun, Y. Wang, X. Shao, X. Xu, F. Cheng, J. Li, and K. Wu, "A unified model: Self-assembly of trimesic acid on gold," *J. Phys. Chem. C* **111**, 10138–10141 (2007).
- ²⁰J. D. Fuhr, A. Carrera, N. Murillo-Quirós, L. J. Cristina, A. Cossaro, A. Verdini, L. Floreano, J. E. Gayone, and H. Ascolani, "Interplay between hydrogen bonding and molecule–substrate interactions in the case of terephthalic acid molecules on Cu(001) surfaces," *J. Phys. Chem. C* **117**, 1287–1296 (2013).
- ²¹C. Glidewell, S. Ahmed, J. Gallagher, and G. Ferguson, "(1'-benzoylferrocenyl)diphenylmethanol; a centrosymmetric R⁴ (16) dimer generated by C–H...O hydrogen bonding," *Acta Crystallogr., Sect. C: Cryst. Struct. Commun.* **53**, 1775–1778 (1997).
- ²²M. Nishio, "The CH/π hydrogen bond in chemistry. Conformation, supramolecules, optical resolution and interactions involving carbohydrates," *Phys. Chem. Chem. Phys.* **13**, 13873–13900 (2011).
- ²³T. Steiner, "Unrolling the hydrogen bond properties of C–H...O interactions," *Chem. Commun.* **1997**, 727–734.
- ²⁴T. Steiner and G. Desiraju, "Distinction between the weak hydrogen bond and the van der Waals interaction," *Chem. Commun.* **1998**, 891–892.
- ²⁵N. A. Wasio, R. C. Quardokus, R. P. Forrest, C. S. Lent, S. A. Corcelli, J. A. Christie, K. W. Henderson, and S. A. Kandel, "Self-assembly of hydrogen-bonded two-dimensional quasicrystals," *Nature* **507**, 86–89 (2014).
- ²⁶R. C. Quardokus, N. A. Wasio, J. A. Christie, K. W. Henderson, R. P. Forrest, C. S. Lent, S. A. Corcelli, and S. A. Kandel, "Hydrogen-bonded clusters of ferrocenecarboxylic acid on Au(111)," *Chem. Commun.* **50**, 10229–10232 (2014).
- ²⁷T. Sammakia and H. Latham, "On the mechanism of oxazoline-directed metalations: Evidence for nitrogen-directed reactions," *J. Org. Chem.* **61**, 1629–1635 (1996).
- ²⁸A. R. Petrov, K. Jess, M. Freytag, P. G. Jones, and M. Tamm, "Large-scale preparation of 1,1'-ferrocenedicarboxylic acid, a key compound for the synthesis of 1,1'-disubstituted ferrocene derivatives," *Organometallics* **32**, 5946–5954 (2013).
- ²⁹Y. Terada, B. Choi, S. Heike, M. Fujimori, and T. Hashizume, "Placing conducting polymers onto a H-terminated Si(100) surface via a pulse valve," *Nano Lett.* **3**, 527–531 (2003).
- ³⁰R. Quardokus, N. Wasio, R. Forrest, C. Lent, S. Corcelli, J. Christie, K. Henderson, and S. Kandel, "Adsorption of diferrocenylacetylene on Au(111) studied by scanning tunneling microscopy," *Phys. Chem. Chem. Phys.* **15**, 6973–6981 (2013).
- ³¹D. Zhong, K. Wedeking, T. Bloemker, G. Erker, H. Fuchs, and L. Chi, "Multilevel supramolecular architectures self-assembled on metal surfaces," *ACS Nano* **4**, 1997–2002 (2010).
- ³²G. Palenik, "Crystal and molecular structure of ferrocenedicarboxylic acid," *Inorg. Chem.* **8**, 2744 (1969).
- ³³F. Takusagawa and T. Koetzle, "Crystal and molecular-structure of 1,1'-ferrocenedicarboxylic acid (triclinic modification)—neutron and x-ray-diffraction studies at 78 K and 298 K," *Acta Crystallogr., Sect. B: Struct. Crystallogr. Cryst. Chem.* **35**, 2888–2896 (1979).
- ³⁴D. Braga, M. Polito, D. D'Addario, and F. Gregioni, "Polymorphism of molecular organometallic crystals. A third form of the supramolecular hydrogen-bonded dimer {[Fe^{II}(η⁵-C₅H₄COOH)₂]₂," *Cryst. Growth Des.* **4**, 1109–1112 (2004).
- ³⁵J. D. Smith, C. D. Cappa, W. S. Drisdell, R. C. Cohen, and R. J. Saykally, "Raman thermometry measurements of free evaporation from liquid water droplets," *J. Am. Chem. Soc.* **128**, 12892–12898 (2006).
- ³⁶W. S. Drisdell, R. J. Saykally, and R. C. Cohen, "On the evaporation of ammonium sulfate solution," *Proc. Natl. Acad. Sci. U. S. A.* **106**, 18897–18901 (2009).
- ³⁷E. Rabani, D. Reichman, P. Geissler, and L. Brus, "Drying-mediated self-assembly of nanoparticles," *Nature* **426**, 271–274 (2003).
- ³⁸R. Deegan, O. Bakajin, T. Dupont, G. Huber, S. Nagel, and T. Witten, "Capillary flow as the cause of ring stains from dried liquid drops," *Nature* **389**, 827–829 (1997).
- ³⁹M. Elbaum and S. Lipson, "How does a thin wetted film dry up," *Phys. Rev. Lett.* **72**, 3562–3565 (1994).
- ⁴⁰B. Teo and N. Sloane, "Magic numbers in polygonal and polyhedral clusters," *Inorg. Chem.* **24**, 4545–4558 (1985).
- ⁴¹M. Bohringer, K. Morgenstern, W. Schneider, R. Berndt, F. Mauri, A. De Vita, and R. Car, "Two-dimensional self-assembly of supramolecular clusters and chains," *Phys. Rev. Lett.* **83**, 324–327 (1999).
- ⁴²N. Kubota, T. Fukuo, and R. Akawa, "Electrospray ionization mass spectrometric analysis of self-assembled 1,1'-ferrocenedicarboxylic acid," *J. Am. Soc. Mass Spectrom.* **10**, 557–560 (1999).
- ⁴³N. Nishi and K. Yamamoto, "Conversion of liquids to cluster beams by adiabatic expansion of liquid jets—mass-spectrometric analysis of molecular association in aqueous-solution systems," *J. Am. Chem. Soc.* **109**, 7353–7361 (1987).
- ⁴⁴N. Nishi, K. Koga, C. Ohshima, K. Yamamoto, U. Nagashima, and K. Nagami, "Molecular association in ethanol water mixtures studied by mass-spectrometric analysis of clusters generated through adiabatic expansion of liquid jets," *J. Am. Chem. Soc.* **110**, 5246–5255 (1988).
- ⁴⁵M. Tjahjono, S. Cheng, C. Li, and M. Garland, "Self-association of acetic acid in dilute deuterated chloroform. Wide-range spectral reconstructions and analysis using FTIR spectroscopy, BTEM, and DFT," *J. Phys. Chem. A* **114**, 12168–12175 (2010).
- ⁴⁶W. Ostwald, "Studies on the formation and transformation of solid bodies," *Z. Phys. Chem.* **22**, 289–330 (1897).
- ⁴⁷T. Threlfall, "Structural and thermodynamic explanations of Ostwald's rule," *Org. Process Res. Dev.* **7**, 1017–1027 (2003).
- ⁴⁸R. Vigil and R. Ziff, "Random sequential adsorption of unoriented rectangles onto a plane," *J. Chem. Phys.* **91**, 2599–2602 (1989).
- ⁴⁹T. Beyer and S. Price, "Dimer or catemer? Low-energy crystal packings for small carboxylic acids," *J. Phys. Chem. B* **104**, 2647–2655 (2000).
- ⁵⁰J. Chen and B. L. Trout, "Computational study of solvent effects on the molecular self-assembly of tetrolic acid in solution and implications for the polymorph formed from crystallization," *J. Phys. Chem. B* **112**, 7794–7802 (2008).
- ⁵¹D. Di Tommaso, "The molecular self-association of carboxylic acids in solution: Testing the validity of the link hypothesis using a quantum mechanical continuum solvation approach," *Crystengcomm* **15**, 6564–6577 (2013).
- ⁵²S. Parveen, R. Davey, G. Dent, and R. Pritchard, "Linking solution chemistry to crystal nucleation: The case of tetrolic acid," *Chem. Commun.* **2005**, 1531–1533.